

Kinetics and Mechanism of Reductive Dioxygen Activation Catalyzed by the P-450 Model System. Iron Picket Fence as a Catalytic Center

Iwao Tabushi,* Masahito Kodera, and Masataka Yokoyama†

Contribution from the Department of Synthetic Chemistry, Kyoto University, Sakyo-Ku, Kyoto, 606 Japan. Received September 24, 1984

Abstract: Picket-fence porphyrin (TpivotP)-iron-*N*-methylimidazole- O_2 complex is used as an artificial P-450, and the decomposition rates are investigated in detail in the presence of HCl and H_2 -colloidal platinum supported on poly(vinylpyrrolidone) with or without addition of benzoic anhydride. From the decay rates of the oxy complex followed by electronic spectrum under a variety of conditions, pseudo-first-order rate (with the complex) constants are obtained. The pseudo-first-order constants are proportional to first order with the colloidal platinum and first order with dihydrogen. Analysis of the dependence of the rate constants on acidity strongly suggests the simultaneous participation of the protonated and unprotonated oxy complexes in the transition states. Cyclohexene used as a guest does not affect the rate at all, demonstrating that the product-forming step comes later than the rate-determining step. It is also ascertained that H_2 favorably competes with cyclohexene in the product-forming step under the conditions of the rate measurements. However, competitive oxidation of the present artificial P-450 porphyrin is satisfactorily slow, and solvent oxidation is not appreciable. Products of the present acid-catalyzed reductive decomposition of the oxy complex are corresponding ferric (deoxy) complex, *trans*-cyclohexan-1,2-diol ethyl ether derived from cyclohexene oxide and ethanol. Slow regeneration of the ferrous oxy complex from the ferric complex leads to the effective recycling (turnover) of the artificial P-450 system.

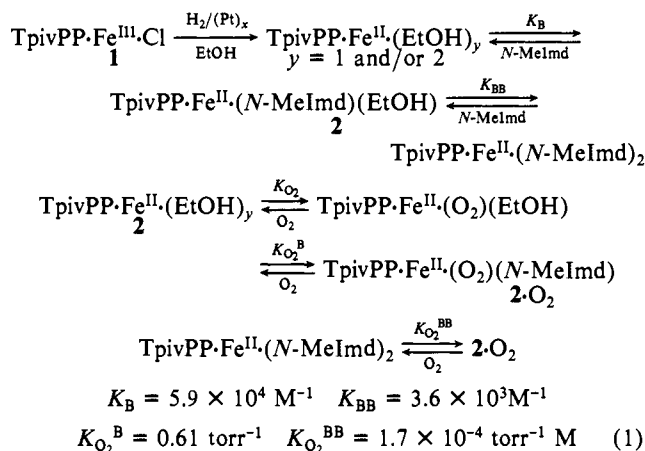
Cytochrome P-450,¹ a typical monooxygenase, has been attracting much interest lately among chemists and biochemists because of its physiological significance and unique mechanism. Among the many unique and novel chemical features of the monooxygenation, the unusual oxidation state of iron Fe(V), the iron oxene structure, and the mechanism of "reductive oxygenation" are especially interesting and important. In order to clarify the structural characteristics of the active species involved in the P-450 cycle, simple model systems have been investigated.² In several of these artificial systems, the iron(V) oxene structure has been successfully prepared by "oxygen atom transfer" from iodosylbenzene and has been satisfactorily characterized spectroscopically.³

Our own efforts have been more concerned with elucidating the mechanism whereby dioxygen is reductively activated. We have found that some typical monooxygenation reactions of dioxygen can be smoothly and efficiently (with high recycling numbers of catalysts) catalyzed by simple model systems consisting of a metalloporphyrin and of dihydrogen in the presence of polymer-supported colloidal platinum.⁴ The reducing reagent, H_2 /col-Pt can be replaced by $NaBH_4$ ⁵ but at the expense of suffering undesired side reactions.⁵

Now we wish to report a detailed kinetic study of the reductive activation of O_2 when using TpivotP-Fe as the catalytic center. Our results suggested that, for dioxygen activation, the model system behaves in a fashion quite similar to that of the native P-450.

Results and Discussion

TpivotP-Fe^{II}-*N*-Methylimidazole⁶ Complex as Artificial P-450. Picket-fence porphyrin⁷ was converted to the Fe^{III} complex, **1**, and further to the artificial P-450 catalytic center, TpivotP-Fe^{II}-*N*-MeImd complex,⁷ **2**, in order to clarify a mechanism of dioxygen activation of the cytochrome P-450 type. On the basis of the observed association constants for the *N*-MeImd ligation and the dioxygen coordination (see eq 1),⁸ the initial concentration of *N*-MeImd and the initial O_2 partial pressure were chosen so that the extent of the conversion from TpivotP-Fe^{II} to **2**· O_2 (see eq 1) was 90–100%. The appropriate *N*-MeImd concentrations and



O_2 partial pressures were found to be 0.182–16.2 × 10⁻⁴ M and 95–380 mmHg, respectively. For the calculation, partial conversion of the free *N*-MeImd to the *N*-MeImd·H⁺ under the reaction conditions was taken into account. The oxy complex, **2**· O_2 , decomposed only slowly in the present solvent, ethanol-toluene (1/2 v/v), at 25 °C in the absence of acid ($\tau_{1/2}$, ca. 1 h; [*N*-MeIm] = 1.15 × 10⁻⁵ M, under 1 atm of dioxygen; see later example in Table I). Added HCl was converted to *N*-MeIm-

(1) Sato, R.; Omura, T. "CYTOCHROME P-450"; Academic Press: New York, San Francisco, London, 1978. White, R. E.; Coon, M. J. *Annu. Rev. Biochem.* **1980**, *49*, 315–356. Guengerich, F. P.; Macdonald, T. L. *Acc. Chem. Res.* **1984**, *17*, 9–16.

(2) Groves, J. T.; Nemo, T. E. *J. Am. Chem. Soc.* **1983**, *105*, 5786–5791, 5791–5796, 6243–6248. Powell, M. F.; Pai, E. F.; Bruce, T. C. *J. Am. Chem. Soc.* **1984**, *106*, 3277–3285.

(3) Groves, J. T.; Haushalter, R. C.; Nakamura, M.; Nemo, T. E.; Evans, B. J. *J. Am. Chem. Soc.* **1981**, *103*, 2884.

(4) (a) Tabushi, I.; Yazaki, A. *J. Am. Chem. Soc.* **1981**, *103*, 7371. (b) Stereospecific, regioselective, and catalytic monoepoxidation of polyolefins and found: Tabushi, I.; Morimitsu, K. *J. Am. Chem. Soc.* **1984**, *106*, 6871–6872.

(5) Tabushi, I.; Koga, N. *J. Am. Chem. Soc.* **1979**, *101*, 6456.

(6) *N*-Methylimidazole was used throughout the experiments. *N*-Methylimidazole is abbreviated as *N*-MeImd in this article.

(7) Collman, J. P.; Gagne, R. R.; Reed, C. A.; Halbert, T. R.; Lang, G.; Robinson, W. T. *J. Am. Chem. Soc.* **1975**, *97*, 1427–1439.

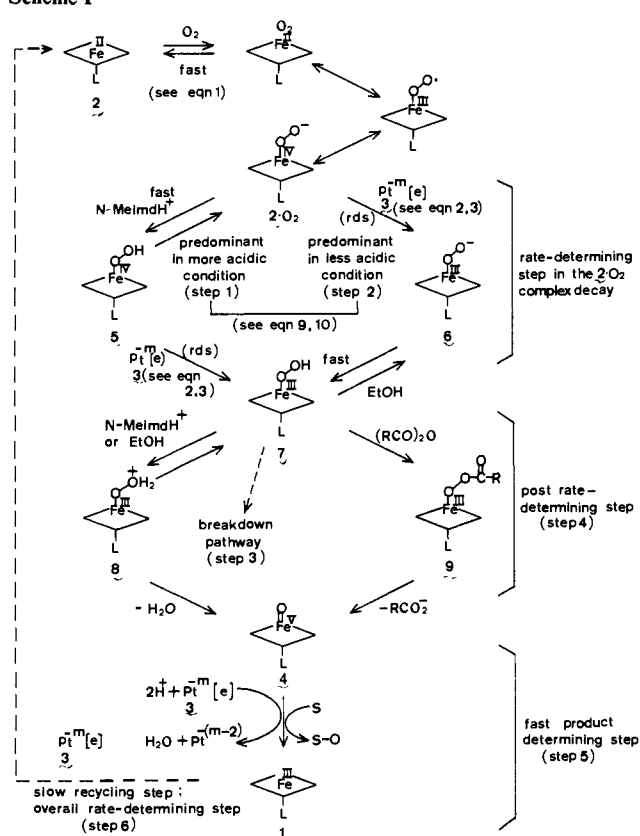
(8) Collman, J. P.; Brauman, J. I.; Doxsee, K. M.; Halbert, T. R.; Suslick K. S. *Proc. Natl. Acad. Sci. U.S.A.* **1978**, *75*, 564–568. Ellis, P. E.; Linard, J. E.; Szymanski, T.; Jones, R. D.; Budge, J. R.; Basolo, F. *J. Am. Chem. Soc.* **1980**, *102*, 1889–1904.

† Department of Chemistry, Faculty of Science, Chiba University, Yayoi-cho, Chiba City 260 Japan.

Table I. Rates of Acid Decomposition of Metalloporphyrin Dioxygen Complex, Rates of Colloidal Pt-Catalyzed Reduction of Metalloporphyrins, and Reductive Acid Decomposition of the Artificial P-450 System

| system (at 25 °C) | solvent | rate constant k , $M^{-1} s^{-1}$ | ref |
|--|-----------|--|-----------|
| TpivPP·Fe ^{II} ·(O ₂)(<i>N</i> -MeIm) | PhMe-EtOH | $1.9 \times 10^{-4}{}^a$ | this work |
| TpivPP·Fe ^{II} ·(O ₂)(<i>N</i> -MeIm)-HCl | PhMe-EtOH | $(4.40 \pm 0.30) \times 10^2{}^b$ | this work |
| TpivPP·Fe ^{II} ·(O ₂)(<i>N</i> -BuIm)-1- <i>n</i> -butylimidazole-HOTs | THF | ca. 2.0 | 7 |
| TPP·Mn ^{III} ·Cl-H ₂ -Pt/PVP | PhH-EtOH | $(8.10 \pm 1.00) \times 10^7{}^c$ | this work |
| TpivPP·Fe ^{III} ·Cl- <i>N</i> -MeIm-H ₂ -Pt/PVP | PhMe-EtOH | $(7.33 \pm 0.50) \times 10^7{}^c$ | this work |
| TpivPP·Fe ^{II} ·(O ₂)(<i>N</i> -MeIm)-H ₂ -Pt/PVP-HCl | PhMe-EtOH | $(1.78 \pm 0.28) \times 10^9{}^d$ | this work |

^a Observed pseudo-first-order rate constant k_{obsd} (s^{-1}); [TpivPP·Fe^{II}·(O₂)(*N*-MeIm)] = 9.10×10^{-6} M, [*N*-MeIm] = 1.15×10^{-5} M, P_{O_2} = 1 atm, at 25 °C. ^b Rate constant calculated on the basis of k_{obsd} values proportional to concentration of hydrochloric acid (see Figure 1). ^c Pseudo-second-order rate constant in (particle equiv/L)⁻¹ s⁻¹; P_{H_2} = 1 atm. ^d Pseudo-second-order rate constant in (particle equiv/L)⁻¹ s⁻¹; H₂/O₂ = 7:1 (v/v); concentrations of *N*-MeIm and HCl were fixed at 1.60×10^{-4} and 3.00×10^{-5} M (see Figure 2).

Scheme I

dH^+Cl^- , since an excess amount of the imidazole was always present under the reaction conditions. In the presence of *N*-MeImdH⁺Cl⁻, the oxy complex $2 \cdot O_2$ decomposed much faster as reported for TpivPP·Fe·(O₂), *N*-*n*-BuIm) in the presence of TsOH in THF,⁷ giving TpivPP·Fe^{III}·Cl⁻ as a sole detectable product (electronic spectrum; 416 and 507 nm⁷). The rate was dependent on the added HCl concentration (see Figure 1 and Table I). The rate constants for the acid-catalyzed decomposition of $2 \cdot O_2$ listed in Table I clearly demonstrate that $2 \cdot O_2$ is still sufficiently stable to allow *usual* rate measurements. However, the addition of H₂/Pt caused a remarkable further acceleration of the decomposition of $2 \cdot O_2$, as discussed later, which was followed only by the stopped-flow technique (see also Scheme I and Table I).

Colloidal Platinum Supported on Polymer as Artificial P-450 Reductase. Colloidal platinum supported on poly(vinylpyrrolidone) (PVP), **3**, was prepared according to the literature.⁹ The efficient

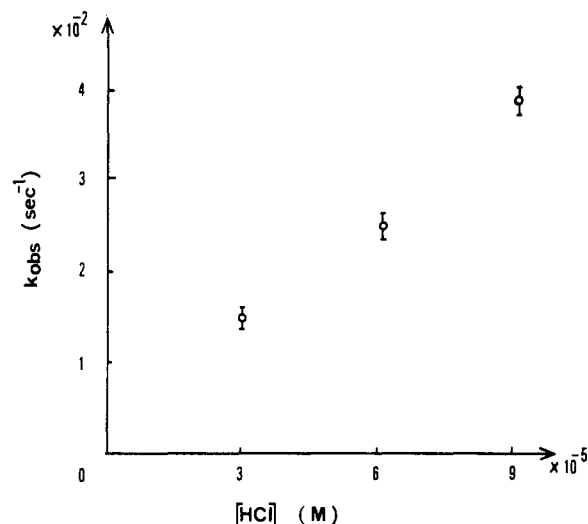
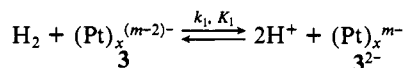
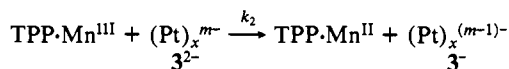


Figure 1. Dependence of pseudo-first-order rate constants for the decomposition of $2 \cdot O_2$ on the added HCl. [HCl] = $(3.00-9.00) \times 10^{-4}$ M, [*N*-MeIm] = 1.60×10^{-3} M, [$2 \cdot O_2$] = 9.10×10^{-6} M, toluene/ethanol = 2:1 (v/v), under atmospheric pressure of air, $T = 25 \pm 0.5$ °C.

conversion of (H^+ + electron) to H₂ by **3** is well-known¹⁰ under a variety of conditions. Furthermore, satisfactory characterization



$$[3^{2-}] = K_1 \frac{[H_2][3]}{[H^+]^2} = K_1' [H_2][3] \text{ at constant pH} \quad (2)$$



(Pt):colloidal platinum supported on PVP;

atom aggregation number, ca. 10^3 .^{9,10}

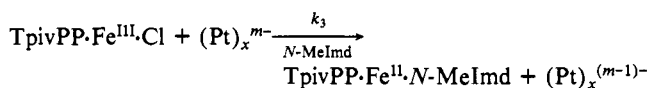
of **2** has been made.⁹ According to the electron micrographic measurements,⁹ colloidal Pt is a spherical particle with ca. 30-Å diameter, or an aggregate of ca. 1000 Pt atoms.^{9,10} Interestingly, however, **3** was also demonstrated by us to be a very efficient catalyst converting H₂ to (electron + H⁺)^{4,10} under a variety of conditions. We therefore conclude that the reduction potential of **3** is very close to that of the H⁺/H₂ couple, -0.421 V NHE at pH 7. According to our preliminary studies, the electron transport activity of **3** discussed above is much higher than the

(9) Hirai, H.; Nakao, Y.; Toshima, N. *J. Macromol. Sci., Chem.* **1979**, *A13*, 727.

(10) Tabushi, I.; Yazaki, A. *J. Org. Chem.* **1981**, *46*, 1899. Tabushi, I.; Yazaki, A. *Tetrahedron* **1981**, *37*, 4185. Kiwi, J.; Gratzel, M. *J. Am. Chem. Soc.* **1979**, *101*, 7214. Brugger, P.-A.; Cuendet, P.; Gratzel, M. *J. Am. Chem. Soc.* **1981**, *103*, 2923.

olefin hydrogenation activity. On the basis of all the information currently available, the H₂/3 system used in our studies seems to be an excellent substitute for the native NADH/P-450 reductase (flavoprotein) couple. The most significant feature of 3 is the large rate constant, *k*₂, for the "digestion" of dihydrogen as has been previously reported by us in preliminary form.¹¹ We have measured the rates of the reduction of TPP·Mn^{III} with H₂/3 by usual stopped-flow electronic spectroscopy (see Table I). The observed rates are reproducible and are taken as the standard for evaluation of the activity of 3. The activity of 3 remained stable during at least 3 days when it was stored in a clean vessel (to avoid any poisoning) and kept in the dark under H₂ atmosphere.

The present artificial P-450 catalytic center, TpvPP·Fe^{III}·Cl⁻, was reduced quantitatively by H₂/3 based on changes in the electronic spectrum. The absorptions at 416, 507, 578, and 650 nm disappear and are replaced by bands newly appeared at 429 and 538 nm. The rate of the reduction was very fast (8 × 10⁷ s⁻¹ M⁻¹; see further Table I) and was proportional to first order of the concentration of TpvPP·Fe^{III}·Cl⁻, dihydrogen (partial pressure), and 3, as shown in eq 3. The second-order rate was



$$v = k_3[\text{TpvPP}\cdot\text{Fe}^{\text{III}}\cdot\text{Cl}][3^{m-}] \quad (3a)$$

$$m = 1 \text{ or } 2$$

$$[3^{m-}] = K_3[3][\text{H}_2]_{\text{soln}} = K_3\alpha[3]P_{\text{H}_2} \quad (3b)$$

$$v = -\frac{d[\text{TpvPP}\cdot\text{Fe}^{\text{III}}\cdot\text{Cl}]}{dt}$$

expressed by eq 3 where [H₂]_{soln} is the concentration of dihydrogen in the solution, P_{H₂} is the partial pressure of H₂, and therefore *v* is proportional to P_{H₂} and [3]. *k*₃ from the observed pseudo-first-order rates is calculated as (7.33 ± 0.50) × 10⁷ (particle equiv/L)⁻¹ s⁻¹ (see below), where estimation of *k*₃ is based on the assumption that every colloidal Pt bears effective negative charge on it ([3]^{m-} ≈ [3]) under the condition. The second-order rate constant, *k*₃, estimated above is the lowest limit of a true *k*₃ value, because of the fact that the negative charge loading on 3 cannot be 100% efficient. Therefore, the present electron-transfer reaction is a very effective one, only 1–2 orders of magnitude slower than the diffusion-controlled limit. As already mentioned, colloidal Pt is a spherical aggregate of ca. 10³ Pt atoms, and, therefore, collision must be described by use of particle equivalents/liter, which corresponds to moles/liter. The large *k*₃ value as well as the "cleanness" (i.e., quantitative conversion from the oxidized to the reduced state without any side reaction) of the catalysis observed suggests that systems derived from 3 are promisingly applied to generate a wide range of artificial "reductase" systems. For instance, the effective and clean reduction of certain native enzymes with the H₂/3 system has been shown¹¹ for cytochrome *c*, cytochrome *c*₃, hemoglobin, myoglobin, or horseradish peroxidase, with second-order rate constants ranging from 10³ to 10⁶ s⁻¹ (particle equiv/L)⁻¹.

Reductive Decomposition of TpvPP·Fe^{II}·(N-MeImd)·(O₂) Facilitated by Colloidal Platinum-H₂. The decomposition of the oxy complex, 2·O₂, in ethanol-toluene (1:2), as followed by stopped-flow electronic spectroscopy, was greatly accelerated in the presence of H₂/3, as shown in Figures 2 and 3 and Table I. This accelerated reductive decomposition gave TpvPP·Fe^{III}·Cl as the sole detectable porphyrin product⁷ in the absence of a substrate molecule. Formation of any intermediate in any detectable amount has never been observed. Therefore, the steady-state concentrations of the intermediates must be low; in other words, a series of steps involved in the further conversion to generate the Fe^{III} species are in fast steps. This point is further discussed in a later section (see further Scheme I). The decomposition rates of 2·O₂ are in accord with a intermolecular rate

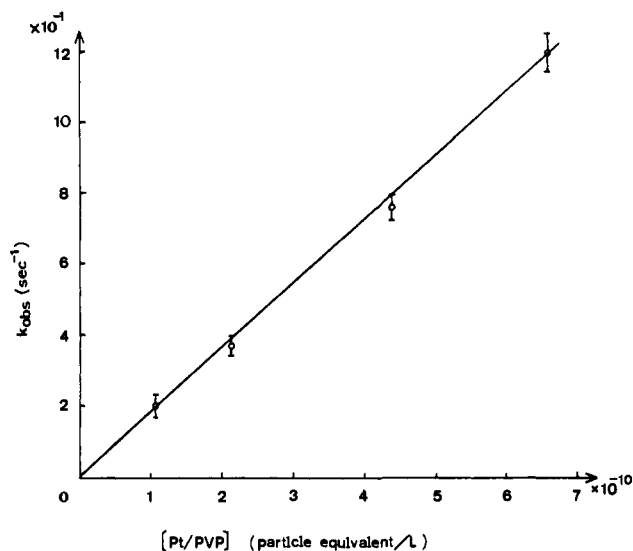


Figure 2. Dependence of pseudo-first-order rate constants for the decomposition of 2·O₂ on the colloidal Pt concentration. [(Pt)_x/PVP] = (1.09–6.57) × 10⁻¹⁰ particle equiv/L, [HCl] = 3.06 × 10⁻⁵ M, [N-MeIm] = 1.60 × 10⁻⁴ M, [2·O₂] = 9.10 × 10⁻⁶ M, H₂/O₂ = 7:1 (v/v), toluene/ethanol = 2:1 (v/v), T = 25 ± 0.5 °C.

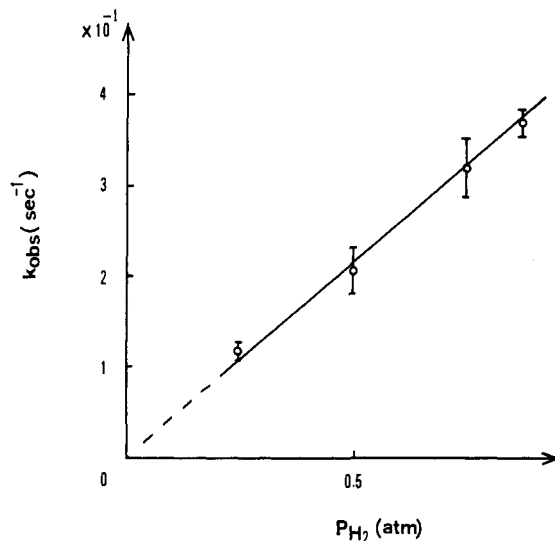
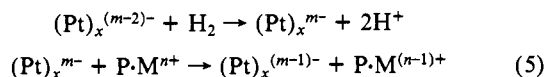


Figure 3. Dependence of pseudo-first-order rate constants for the decomposition of 2·O₂ on H₂ partial pressure. H₂ and O₂ were diluted with N₂. Total pressure is 1 atm. Volume ratios of mixed gases are as follows: H₂/O₂/N₂ = 1:1:6, 2:1:5, 4:1:3, 7:1:0 (v/v). [N-MeIm] = 1.60 × 10⁻⁴ M, [HCl] = 3.06 × 10⁻⁵ M, [(Pt)_x/PVP] = 2.19 × 10⁻¹⁰ particle equiv/L, toluene/ethanol = 2:1 (v/v), [2·O₂] = 9.10 × 10⁻⁶ M, T = 25 ± 0.5 °C.

expression, being proportional to first order in the concentration of the oxy complex 2·O₂, the colloidal Pt 3, and the partial pressure of H₂, as shown in eq 4 where [H₂]_{soln} denotes the concentration

$$-\frac{d[2\cdot\text{O}_2]}{dt} = k_4[2\cdot\text{O}_2]\cdot[3]\cdot P_{\text{H}_2} = k_4'[2\cdot\text{O}_2]\cdot[3]\cdot[\text{H}_2]_{\text{soln}} \quad (4)$$

of dihydrogen in the present solvent system. The most plausible mechanism of the electron-transfer catalysis of 3 to interpret its unique characteristics discussed above may be



(Pt)_x: colloidal platinum, *x* ≈ 1000

m - 2: zero or other integers

Effect of Acidity and Acid Anhydride in Post-Rate-Determining Steps. Artificial Cofactor. In the native P-450 catalysis, pro-

(11) Tabushi, I.; Nishiyama, T. *J. Am. Chem. Soc.* **1981**, *103*, 6963.

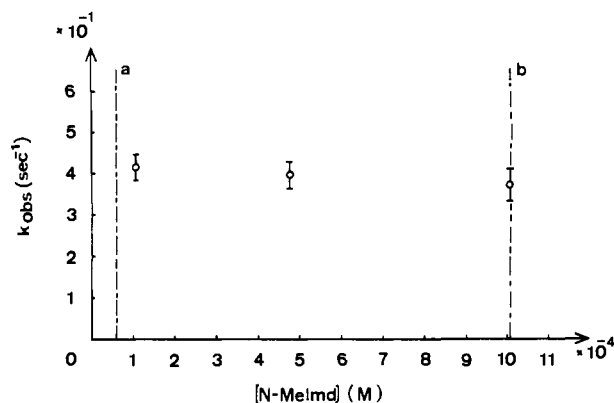
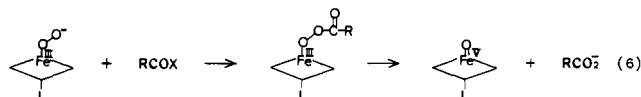


Figure 4. Dependence of pseudo-first-order rate constants for the decomposition of $2\cdot\text{O}_2$ on total *N*-methylimidazole concentration. The ratio of concentration of *N*-methylimidazole to that of HCl is kept constant. $[\text{N-MeIm}]/[\text{HCl}] = 2.7$ (M/M), $[\text{N-MeIm}] = (1.82\text{--}16.2) \times 10^{-4}$ M, $[\text{HCl}] = (0.60\text{--}6.0) \times 10^{-4}$ M, $[(\text{Pt})_x/\text{PVP}] = 2.19 \times 10^{-10}$ particle equiv/L, $[2\cdot\text{O}_2] = 9.10 \times 10^{-6}$ M, $\text{H}_2/\text{O}_2 = 1:1$ (v/v), toluene/ethanol = 2:1 (v/v), $T = 25 \pm 0.5$ °C. In the region of $a \leq [\text{N-MeImd}] \leq b$, $[2\cdot\text{O}_2] \geq 93\%$. Values of a and b were determined spectrophotometrically in toluene-ethanol.

tonation has been assumed as being one of the key steps in the O_2 -activation process.¹ Recently, however, lipoic acid was shown to be a cofactor in the P-450 O_2 activation.¹² In the artificial P-450 systems, detailed information has not yet been available on the acidity-rate profile. In some model systems previously studied, metal acylperoxy complexes were shown to give metal oxene-type intermediates based on the magnetic moment at -78 °C, NMR, and electronic spectra.^{3,13} A plausible mechanism interpreting the role of the cofactor and the acylperoxy intermediate is shown in eq 6. Considering these, we have investigated



the acidity-rate profile and effect of benzoic anhydride as a possible acylating reagent on the rate for our present artificial P-450 system. For the investigation of the acidity-rate (rate of the decrease of the complex $2\cdot\text{O}_2$) profile, a buffer system consisting of *N*-MeImd- $\text{H}^+\text{Cl}^-/\text{N-MeImd}$ was used to adjust the acidity. For this purpose, the effect of the *N*-MeImd concentration on the rates was first studied by keeping the *N*-MeImd- $\text{H}^+\text{Cl}^-/\text{N-MeImd}$ ratio constant as a stable buffer system. The results show that the rate is not substantially affected by the imidazole concentration except at very low concentrations (see Figure 4) where the formation of $2\cdot\text{O}_2$ is incomplete. Formation of $2\cdot\text{O}_2$ was directly observed by the use of electronic spectrum (430 nm), being 95 and 93% at the *N*-MeImd concentrations of 1.2×10^{-3} and 1.0×10^{-3} M, respectively. Therefore, we conclude that the *N*-MeImd accelerates the overall rate only via coordination to the iron (see region a-b in Figure 4) to increase the concentration of $2\cdot\text{O}_2$ and that any further effect of *N*-MeImd, either as a base or a nucleophile, on the rate is negligible.

The acidity was adjusted by changing the HCl concentration at the constant total *N*-MeImd concentration. The acidity function was determined spectrophotometrically by using papaverine as an indicator.¹⁷ The logarithmic pseudo-first-order rate constant of the decrease of $2\cdot\text{O}_2$ was approximately proportional to the

(12) Sligar, S. G.; Kennedy, K. A.; Pearson, D. C. *Proc. Natl. Acad. Sci. U.S.A.* **1980**, *77*, 1240.

(13) Groves, J. T.; Watanabe, Y.; McMurry, T. J. *J. Am. Chem. Soc.* **1983**, *105*, 4489.

(14) Careful adjustment of the dioxygen partial pressure gives an equimolar mixture of the corresponding deoxy and oxy complexes. The mixture does not show any appreciable spectral change under the conditions of the present rapid rate measurements.

(15) Under the conditions, the observed recycling number of **1** for $\text{H}_2\text{--O}_2$ reaction is 1.3×10^3 (number of H_2 molecule oxidized/number of **1** used).

(16) Mansuy, D.; Leclaire, J.; Fontecave, M.; Momenteau, M. *Biochem. Biophys. Res. Commun.* **1984**, *119*, 319-325.

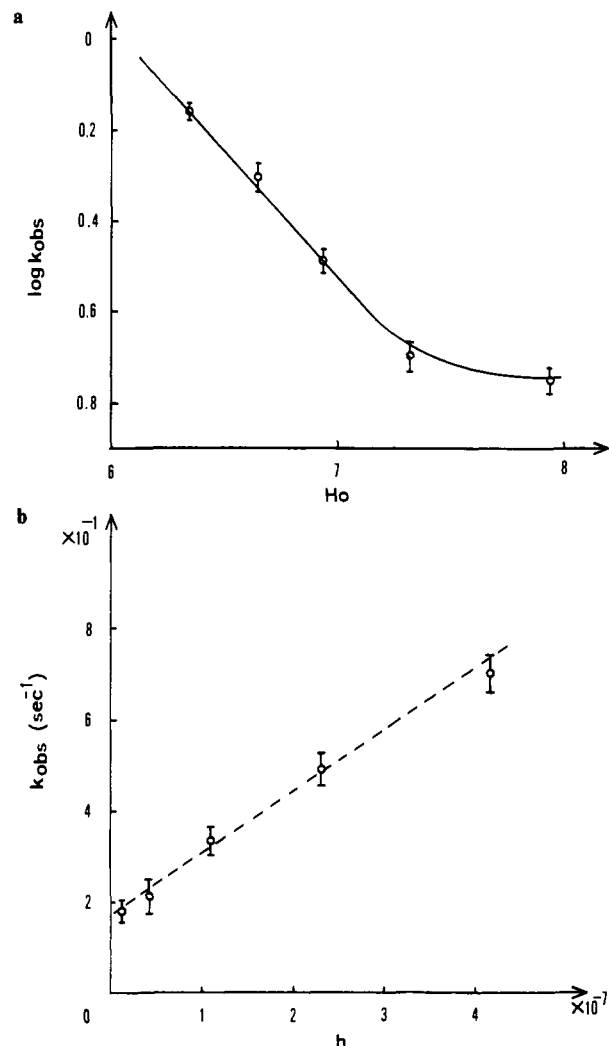


Figure 5. Dependence of observed pseudo-first-order rate constants for the decomposition of $2\cdot\text{O}_2$ on the acidity (a, top) vs. the acidity function, H_0 and (b, bottom) vs. the acidity function, h . Acidity functions H_0 and h were determined by the usual spectroscopic method according to Hammett's definition,¹⁷ where papaverine hydrochloride ($\text{p}K_a = 6.40$) was used as an indicator. $H_0 = \text{p}K_a - \log \{[\text{papaverine HCl}]/[\text{papaverine}]\}$; $H_0 = -\log h$. Concentration of papaverine HCl was determined by the observed absorbance at 344 nm with an electronic spectrophotometer. Total papaverine concentration is 1.00×10^{-4} M. Values of H_0 and h thus determined are given in Table V. Other conditions for kinetic experiments are as follows: $[(\text{Pt})_x/\text{PVP}] = 2.19 \times 10^{-10}$ particle equiv/L, $[2\cdot\text{O}_2] = 9.10 \times 10^{-6}$ M, $\text{H}_2/\text{O}_2 = 1:1$ (v/v), toluene/ethanol = 2:1 (v/v), $T = 25 \pm 0.5$ °C.

acidity function H_0 in the high acidity region (observed slope was -0.57) showing *formally* that a "half"-protonated species was involved in the transition state. However, when acidity decreases, slopes approach zero as shown in Figure 5a. In other words, protonated species as well as unprotonated species may be involved in the rate-determining step. This is further discussed in the last section (see further eq 10 and Scheme I). The complex kinetic behavior at low acidity is due to larger contribution from the unprotonated $2\cdot\text{O}_2$ complex. By the use of another acidity function, h , to denote the "protonation" capacity directly, dual mechanism via protonated and unprotonated $2\cdot\text{O}_2$ becomes clearer (Figure 5b). Decomposition of the corresponding unprotonated μ -peroxy dimer is unlikely because of the observed kinetic order (first order with respect to the porphyrin) and of the independent

(17) Hammett, L. P.; Deyrup, A. J. *J. Am. Chem. Soc.* **1932**, *54*, 2721-2739. Efficient catalytic hydroxylation of aromatic compounds will be reported soon in a separate paper: Tabushi, I.; Morimitsu, K., unpublished results.

(18) Mansuy, D.; Fontecave, M.; Bartoili, J.-F., *J. Chem. Soc., Chem. Commun.* **1983**, 252.

Table II. Observed Recycling Number of Metalloporphyrin in Artificial P-450 Type Catalysis

| metalloporphyrins | recycling number (%) ^d | | substrate | metalloporphyrin consumption (%) at the designated recycling no. |
|---|-----------------------------------|--|-------------|--|
| | mol prod/ mol catal used | mol prod/mol catal consumed (theoret recycling no.) | | |
| TPP·Mn ^{III} ·Cl ^a | 69 | 173 | cyclohexene | 40 |
| TPP·Mn ^{III} ·Cl ^a | | | dihydrogen | 70 |
| TpivPP·Fe ^{II} ·(O ₂)(<i>N</i> -MeImd) ^b | 8 | 11 | cyclohexene | 70 |
| | 900 | | dihydrogen | |
| TpivPP·Fe ^{II} ·(O ₂)(<i>N</i> -MeImd) ^b | | | none | |
| | 650 | | dihydrogen | 90 |
| TPPS ₄ ·Mn ^{III} ·C | 144 | 533 | nerol | 27 |

^aIn the presence of H₂, (Pt)_x/PVP, O₂, and *N*-MeImd in benzene-ethanol. ^bIn the presence of H₂, (Pt)_x/PVP, O₂, and *N*-MeImd in toluene-ethanol. In the presence of cyclohexene (2.8 × 10⁻¹ M), H₂, and O₂ consumptions are 28 and 14 mL, respectively. Other reaction conditions are [TpivPP·Fe^{II}·(O₂)(*N*-MeImd)] = 3.9 × 10⁻⁵ M, [*N*-MeImd] = 1.6 × 10⁻³ M, [HCl] = 1.2 × 10⁻³ M, [(Pt)_x/PVP] = 1.3 × 10⁻⁷ particle equiv/L, H₂/O₂/N₂ = 1:1:1, toluene/ethanol = 1:1 (v/v), reaction time 30 min. ^cIn the presence of H₂, (Pt)_x/PVA, O₂, and *N*-MeImd in H₂O-ethanol; TPPS₄ is tetraphenylporphyrinetetrasulfonic acid. ^dRecycling number is mole of oxygenated products on mole of metalloporphyrin used.

Table III. Products of Artificial P-450 Monooxygenation^a

| <i>N</i> -MeIm, μmol | HCl, μmol | Pt/PVP, particle equiv | TpivPP·Fe ^{II} , μmol | (PhCO) ₂ O, mmol |  mmol | time, min | yield, ^b % | |
|-------------------------|--------------|---------------------------|-----------------------------------|--------------------------------|--|--------------|---|---|
| | | | | | | |  |  |
| 29.2 | 20.9 | 2.3 × 10 ⁻⁹ | 0.7 | | 5 | 30 | 750 | 50 ^c |
| 29.2 | 20.9 | 2.3 × 10 ⁻⁹ | 0.7 | | 0.5 | 30 | 150 | 20 |
| 146 | 104 | 2.3 × 10 ⁻⁹ | 0.7 | | 5 | 30 | 800 | 80 |
| 29.2 | 20.9 | 4.6 × 10 ⁻¹² | 0.7 | | 5 | 1/6 | 5 | |
| 29.2 | 20.9 | 2.3 × 10 ⁻⁹ | 0.7 | 0.5 | 5 | 30 | 1800 | 800 ^c |
| 29.2 | 20.9 | 4.6 × 10 ⁻¹² | 0.7 | 0.5 | 5 | 1/6 | 10 | 1 |
| 29.2 | 20.9 | 2.3 × 10 ⁻⁹ | 0.7 | | 5 | 30 | 0 | 0 |

^aToluene-ethanol (2:1, v/v, 18 mL) was used as a solvent. ^bYields are based on TpivPP·Fe^{II} used. ^cCyclohexane (0.8 μmol) was also produced.

measurements showing unfavorable formation of the μ -peroxy dimer under the present conditions.¹⁴ Most likely, mechanisms for the protonated and unprotonated routes are shown in Scheme I in the last section. The very much facilitated rate-determining electron transfer to the protonated oxy complex (step 1, Scheme I) is reasonably understood on the basis of the increased electron affinity. Electron transfer to the unprotonated oxy complex (step 1) may be facilitated by the solvation and/or the general acid catalysis by ethanol. Rapid protonation after the electron transfer (step 2) is reasonably understood on the basis of the increased basicity.

In the low acidity condition, the corresponding μ -oxo dimer was gradually accumulated as the major product from the porphyrin, (417 and 574 nm⁷), suggesting significant contribution of the reaction between the P-450-type intermediate 4 and the deoxy complex 2.

Addition of benzoic anhydride (0.514–5.14 × 10⁻³ M) accelerates the overall pseudo-first-order rate of the 2·O₂ decrease [$k_{\text{obsd}} = (2.30 \pm 0.25) \times 10^{-1} \text{ s}^{-1}$] only slightly, if any. In the absence of (PhCO)₂O, $k_{\text{obsd}} = (2.08 \pm 0.32) \times 10^{-1} \text{ s}^{-1}$ was obtained ([TpivPP·Fe^{II}·(O₂)(*N*-MeIm)] = 9.10 × 10⁻⁶ M, [*N*-MeIm] = 1.60 × 10⁻⁴ M, [Pt/PVP] = 2.19 × 10⁻¹⁰ particle equiv/L, [HCl] = 3.00 × 10⁻⁵ M, H₂/O₂ = 1:1 (v/v)).

The yield of the epoxide derivative increased by a factor of 2.4 by the addition of 5.0 × 10⁻⁴ M of benzoic anhydride (see Table III). These observations demonstrate that acylation takes place after the rate-determining step in the O₂ activation, facilitating formation of the oxene-active intermediate (eq 6) and minimizing any side breakdown pathway from FeOOH (see Scheme I, step 3). This unidentified competition reaction is involved in the fast step, and, therefore, the addition of benzoic anhydride does not affect the observed rate. By the same reason, steady-state concentrations of the intermediates are too low to be studied spectroscopically.

Fast Product-Determining Step. Competition between Olefinic Substrate and Dihydrogen. In the transition state of the acid-dependent decomposition of 2·O₂ discussed above (Scheme I, step 1), one electron and one proton are involved together with 2·O₂. Therefore, further protonation and water elimination or acylation

followed by deacyloxylation must be involved after the rate-determining step (Scheme I, step 4). A plausible intermediate coming after these steps is the iron oxene 4, which then reacts with cyclohexene to give the epoxide as discussed in the following section. However, there are several candidates which are po-



tentially capable of accommodating atomic oxygen—ligand, metalloporphyrin, reductant, and solvent. No oxidation products from solvent or ligand have ever been detected, and the yield of the main product (cyclohexanediol derivative) has never been appreciably affected by the ligand concentration when it is higher than 0.3 × 10⁻⁴ M (Table III). When cyclohexene was absent, 1 or another metalloporphyrin was seriously destroyed during the present reaction conditions¹⁵ (95% decomposition based on the electronic spectrum of $\tau_{1/2}$ was ca. 6.7 min). Under the analogous conditions but with higher cyclohexene concentration (2.78 × 10⁻² M), the recycling number was ca. 8 (mol product/mol catalyst used) and the observed decay of the metalloporphyrin was 70% after 0.5 h ($\tau_{1/2}$ ca. 11 min, see Table II). The porphyrin decomposition rate in the presence of cyclohexene in the above concentration is slightly less than half of that in the absence of cyclohexene. Therefore, we conclude that metalloporphyrin oxidation is competing with the epoxidation of cyclohexene, only very unfavorably ($k(\text{cyclohexene})/k(\text{porphyrin}) = \text{ca. } 11.4$). Large excess of alkene over porphyrin used naturally makes the porphyrin decomposition much less favorable under the present conditions, and a high recycling number was obtained (see Table II).

The most important competing reaction in the product-determining step (Scheme I, step 5) under the conditions is the deoxygenation of the P-450-type active species (4, Scheme I) by the electron rich colloidal platinum 3^{m-} (eq 7). Under the conditions

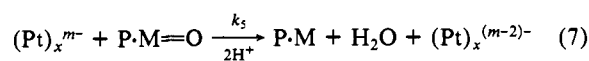
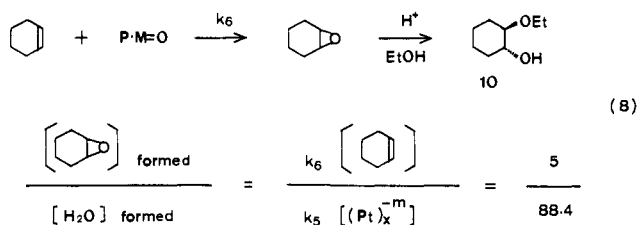


Table IV. Comparison of Epoxidation with Allylic Oxidation

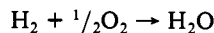
| monooxygenation systems | yield, ^a % | | rel reactivity | ref |
|--|-----------------------|-----------------------|----------------|-----------|
| | epoxidation | allylic oxidation | | |
| TPP·Mn ^{III} ·Cl-H ₂ -Pt/PVP-O ₂ -N-MeIm-cyclohexene | 6500 | 440 | 15/1 | 4 |
| TPP·Mn ^{III} ·Cl-ascorbate-O ₂ -cyclohexene | 230 | not determined | | 18 |
| TPP·Fe ^{III} ·Cl-iodosylbenzene-cyclohexene | 743 (55) ^b | 203 (15) ^b | 3.7/1 | 2 |
| TpivPP·Fe ^{II} ·(O ₂)-(N-MeIm)-H ₂ -Pt/PVP-cyclohexene | 750 | 50 | 15/1 | this work |
| enzyme-6-phenoxyhex-1-ene | 3.4 ^c | 0.65 ^c | 5.2/1 | 16 |

^aYield based on metalloporphyrins used. ^bYield based on iodosylbenzene consumed. ^cFormation rate (nmol·nmol P-450⁻¹·min⁻¹) was shown in place of yield.

specified in Table III, the amount of **10**, the product derived from the epoxide that was measured by GLC, at the 93.4% conversion ($2\text{-O}_2 \rightarrow \mathbf{1}$) level (after 10 s), conditions under which the regeneration of **2** from **1** thus produced via the relatively slow reduction with H₂/colloidal Pt, is still very small (estimated as only 5.5% of the total porphyrin based on the k_3 value of the overall rate controlling reduction—see Scheme I, step 6). Thus, the products observed here are mainly derived from a single cycle of the present conversion from 2-O_2 to **1**. The observed yield of **10** based on 2-O_2 used under the condition was 5.0%, giving the reactivity ratio of 5/88.4 by considering that the 2-O_2 consumed is 93.4% based on the 2-O_2 used. It is concluded, therefore, that the major reaction



pathway in the fast product-determining step under the present conditions is the dihydrogen-dioxygen reaction catalyzed by the metalloporphyrin colloidal platinum. Epoxidation followed by



the ring opening is the second most important pathway. Other side reactions are not important at all, as already discussed.

Product Analysis. The products of the reaction were carefully analyzed by GLC, IR, and NMR. These products were obtained under *recycling* (catalytic) conditions where a large excess of the H₂-O₂ 1:1 mixture was used, and the reaction was allowed to proceed more than 1.22×10^4 kinetic half-lives of the regeneration ($\mathbf{1} \rightarrow \mathbf{2}$, judging from the independent observed rates for the conversion: $\mathbf{1} \rightarrow \mathbf{2}$ (Scheme I, step 6)). The results are listed in Table III. The major reaction pathway for cyclohexene is epoxidation followed by ring opening, but allylic oxidation also occurred to a minor extent, just as in the enzymatic or other artificial systems (Table IV).¹⁵

Rate Equation and Total Mechanism of Dioxygen Activation by Artificial P-450 System. Based on the kinetic measurements described above, the rate expression for the present artificial P-450 system was obtained as eq 9. The first-order dependence on the

$$-\frac{d[2\text{-O}_2]}{dt} = k\lambda[2\text{-O}_2][(\text{Pt})_x][\text{H}_2] \quad (9)$$

2-O_2 concentration was ascertained as shown in Figure 6. λ comes

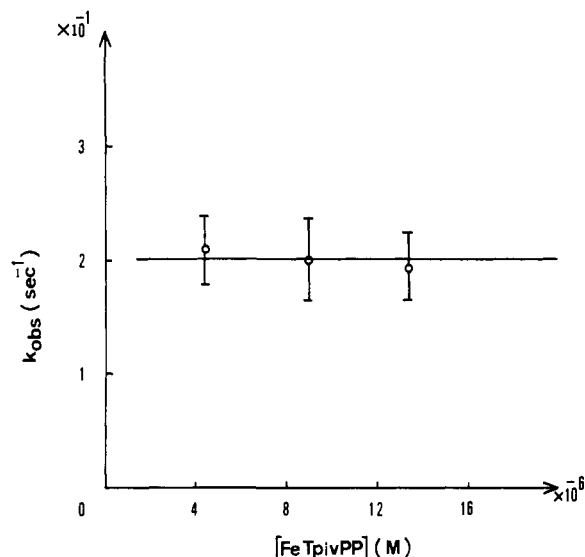


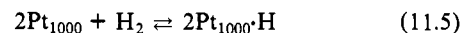
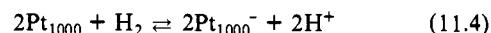
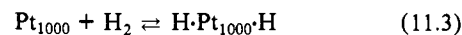
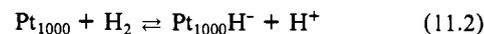
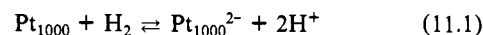
Figure 6. Pseudo-first-order rate constants for the decomposition of 2-O_2 independent of the 2-O_2 concentration. $[2\text{-O}_2] = (4.55\text{--}13.5) \times 10^{-6}$ M, $[N\text{-MeIm}] = 1.60 \times 10^{-4}$ M, $[\text{HCl}] = 3.06 \times 10^{-5}$ M, $[(\text{Pt})_x/\text{PVP}] = 2.19 \times 10^{-10}$ particle equiv/L, H₂/O₂ = 1:1 (v/v), toluene/ethanol = 2:1 (v/v).

from the complex rate dependence on h (acidity) and is approximated as

$$\lambda = h + \text{constant} \quad (10)$$

where $-\log h = H_o$, demonstrating that h (protonation capability) is close to proton activity in an aqueous solution (see Figures 5 and 6). Equation 10 strongly suggests that there are two entirely different reaction mechanisms involved in the present P-450-type O₂ activation—(i) in slightly basic condition, the rate-determining electron transfer to the unprotonated oxy complex is predominant, but (ii) with an increase in the acidity (via the imidazolium concentration increase), the contribution of another mechanism, the acid-catalyzed route, increases as shown in Scheme I, step 1.

The rate dependence with respect to both the colloidal Pt and H₂ concentrations strongly suggests that the active reductant must be formed by a one-to-one reaction between the two species as shown in eq 11.1–11.3. At higher Pt concentrations, however,



a slight upward deviation from linear relationship was observed, suggesting that a contribution from another mechanism [(11.4) or (11.5)] is also occurring to a minor extent. In this stage, information is not enough to determine the most predominant mechanism among (11.1) to (11.3).

The present electron-transfer catalyst, polymer-supported colloidal platinum, “digest” H₂ and digestion of H₂ by colloidal platinum formally provides two electrons on a single platinum particle. One must be consumed by the rate-determining reduction, but the other may be consumed by other processes including the nonproductive oxygen reduction (**4**, Scheme I).

On the basis of our knowledge of the mechanism for the present artificial P-450 system, especially by the use of correlationship between rates and acidity, reductant, or a cofactor, a remarkable and significant improvement in the epoxidation and aromatic hydroxylation conditions by the use of the corresponding Mn species has been made. These findings are reported in an upcoming article.^{4b,17}

Experimental Section

Apparatus. ^1H NMR spectra were recorded on a JEOL PMX-60 spectrophotometer. Chemical shifts are given in δ values from Me_4Si . Electronic absorption spectra were measured with a Union Giken high-sensitivity spectrophotometer SM 401 thermostated at 25.0 ± 0.5 °C with a circulating system, Type Handy Cooler TRL-108.

GLC analysis of the oxygenation products was carried out by using a Shimadzu GC-8A gas chromatograph on a poly(ethylene glycol) column (3 mm diameter \times 2 m, 150 °C, N_2 carrier 1.5 kg/cm 2) and a SE-30 column (3 mm diameter \times 2 m, 150 °C, N_2 carrier 1.0 kg/cm 2).

Vapor pressures of H_2 , O_2 , and N_2 were determined by gas chromatography, by using a Shimadzu GC 4B-IT gas chromatograph on a molecular sieve 13X column (3 mm diameter \times 2 m, 20 °C, Ar carrier 0.5 kg/cm 2).

Materials. Toluene was freed from sulfur-containing compounds by first shaking with cold concentrated H_2SO_4 (100 mL of acid per 1 L of toluene) twice; then it was washed once with water, once with aqueous NaHCO_3 (5%), again once with water, and then dried with anhydrous MgSO_4 . Finally, pure toluene was obtained by fractional distillation from P_2O_5 . Toluene thus purified was stored under dry Ar.

Ethanol was dried with magnesium and then fractionally distilled. Distilled ethanol was stored under dry Ar.

Commercially available PVP (poly(vinylpyrrolidone), M_w 40000) and K_2PtCl_4 were used for preparation of colloidal platinum. The resultant colloidal solution can be kept under H_2 gas for 3 days without appreciable deactivation or precipitation.

An ethanolic solution of HCl was prepared by bubbling dry HCl gas through dry ethanol. HCl gas was generated from concentrated HCl and concentrated H_2SO_4 and dried by passing through concentrated H_2SO_4 . The ethanolic solution of HCl was titrated with 0.100 N aqueous NaOH and then stored in a sealed vessel.

N-Methylimidazole was dried with sodium metal⁸ and then distilled (bp 83–84 °C/27 mmHg). The dry *N*-methylimidazole was stored in a refrigerator under dry Ar. Cyclohexene was refluxed with MeMgI in ether (0.1 mol of MeMgI per 1 mol of cyclohexene) to remove any alcohol, hydroperoxide, or ketone and then fractionally distilled. Cyclohexene, free from the autoxidation impurities, was stored in the refrigerator under dry Ar.

Colloidal Platinum Supported on PVP (Pt/PVP). PVP (30 mg) was dissolved in freshly distilled ethanol (11 mL), and the solution was stirred vigorously with a magnetic stirrer bar at reflux. To this solution was added dropwise an aqueous solution (0.2 mL) of K_2PtCl_4 (10.5 mg). Within 15 min, the solution became dark brown, and the refluxing was continued for additional 2 h. The Pt/PVP solution thus prepared was kept under H_2 gas at room temperature. The catalytic activity of Pt/PVP was checked just before use by measuring the reduction rate of $\text{TPP}\cdot\text{Mn}^{\text{III}}\cdot\text{Cl}$ in the presence of dihydrogen as described below. All glassware were used after washing with aqua regia and distilled water repeatedly.

Reduction of $\text{TPP}\cdot\text{Mn}^{\text{III}}\cdot\text{Cl}$ with Dihydrogen Catalyzed by Colloidal Platinum (Activity Checking Procedure). A 3-mL solution of $\text{TPP}\cdot\text{Mn}^{\text{III}}\cdot\text{Cl}$ (4.2×10^{-6} M) in benzene–ethanol (2:1 v/v) was placed in a quartz cell equipped with a three-way stopcock, and the solution was deaerated by evacuation and refilling with H_2 (10 cycles) and was shaken carefully. To the solution saturated with dihydrogen thus prepared, 0.5 mL of benzene–ethanol (2:1, v/v) solution (saturated with H_2 by the same method described above) containing Pt/PVP ($4.5\text{--}13.5 \times 10^{-13}$ particle equiv) was added with a specially designed syringe¹¹ through a rubber seal attached to the top of the three-way stopcock. The decrease of $[\text{TPP}\cdot\text{Mn}^{\text{III}}\cdot\text{Cl}]$ was monitored at 469 nm with the electronic spectroscopy. Quantitative conversion of the Mn^{III} to the corresponding Mn^{II} complex was observed. Under these conditions, the second-order rate constant was determined to be $(8.1 \pm 1.0) \times 10^7$ (particle equiv/L) $^{-1}$ s $^{-1}$ at 25 ± 0.5 °C. This value is taken as the standard activity of the colloidal Pt.

Preparation of $\text{TpivPP}\cdot\text{Fe}^{\text{II}}(\text{N-MeIm})_2$. H_2TpivPP was prepared by the reported procedure.⁷ The purity of H_2TpivPP is checked by TLC and ^1H NMR: ^1H NMR (CDCl_3) δ 0.05 (s, 36 H), 7.1–8.1 (m, 18 H), 8.7 (s, 4 H), 8.9 (s, 8 H).

In a 50-mL pear-shaped flask equipped with a three-way stopcock were placed 0.8 mL of H_2O and 12 mL of a benzene solution of $\text{TpivPP}\cdot\text{Fe}^{\text{II}}\cdot\text{Cl}$ (0.2 g) containing *N*-methylimidazole (0.8 g). After careful removal of dioxygen by repeated freeze–pump–thaw cycles, the flask was placed in a vacuum box filled with Ar. $\text{Na}_2\text{S}_2\text{O}_4$ (1.6 g) was added to the mixture, and the mixture was stirred with a magnetic stirrer for 30 min. The color of the reaction mixture changed from dark brown to red–brown (visible spectrum change; 417, 507 to 432, 537 nm). The reaction mixture was then treated with anhydrous Na_2SO_4 for 10 min, and solid was filtered off. Upon the addition of dioxygen-free (obtained by repeated freeze–pump–thaw cycles) hexane (40 mL) to the filtrate, purple crystals of $\text{TpivPP}\cdot\text{Fe}^{\text{II}}(\text{N-MeIm})_2$ were obtained. The crystals

collected were dried in vacuo and stored in a vacuum box under Ar.

Preparation of $\text{TpivPP}\cdot\text{Fe}^{\text{II}}(\text{O}_2)(\text{N-MeIm})_2$. $\text{TpivPP}\cdot\text{Fe}^{\text{II}}(\text{N-MeIm})_2$ (12 mg) was dissolved in 25 mL of toluene, the solution was mixed with a toluene solution of *N*-methylimidazole (12.8 mg), and the resultant solution was diluted with toluene to the desired concentration. The diluted solution (2 mL) was mixed with ethanol (1 mL), and Ar gas was replaced by flushing with a mixture of $\text{H}_2\text{--O}_2$ gas [(1–7):1 v/v]. Immediately, $\text{TpivPP}\cdot\text{Fe}^{\text{II}}(\text{O}_2)(\text{N-MeIm})_2$ was formed (visible spectrum 420, 544 nm). The concentration of the iron picket-fence porphyrin complex, the concentration of *N*-methylimidazole, and the partial pressure of O_2 were chosen so that at least 80% conversion to the $\text{TpivPP}\cdot\text{Fe}^{\text{II}}(\text{O}_2)(\text{N-MeIm})_2$ complex occurred.

Rate Measurements. General Procedure of Rate Measurements. A toluene–ethanol (2:1 v/v, 7.5 mL) solution containing HCl and Pt/PVP of desired concentrations was prepared in a small glass vessel equipped with a three-way stopcock, and the solution was saturated with $\text{H}_2\text{--O}_2$ [(1–7):1] by repeated evacuation followed by back-flushing (5 times).

A toluene–ethanol (2:1 v/v, 3 mL) solution of $\text{TpivPP}\cdot\text{Fe}^{\text{II}}(\text{N-MeIm})_2$ was placed in a quartz-cell previously degassed and filled with Ar. The cell was equipped with a three-way stopcock, through which a $\text{H}_2\text{--O}_2$ [(1–7):1] gas mixture was introduced by the same procedure as described above.

The iron porphyrin solution was mixed with the platinum solution prepared as described previously by use of a stopped-flow syringe.¹¹ The decrease of $\text{TpivPP}\cdot\text{Fe}^{\text{II}}(\text{O}_2)(\text{N-MeIm})_2$ was followed by monitoring the change in the visible absorption at 544 nm. Rapid and quantitative conversion of the $\text{TpivPP}\cdot\text{Fe}^{\text{II}}(\text{O}_2)(\text{N-MeIm})_2$ to $\text{TpivPP}\cdot\text{Fe}^{\text{III}}\cdot\text{Cl}$ was observed. However, in the very low acidic condition, the μ -oxo dimer (417, 574 nm in EtOH/toluene) was accumulated. Estimations of k_{obsd} were made by plotting the logarithms of the absorbance change vs. time. All kinetic experiments were carried out under pseudo-first-order conditions, and several independent kinetic runs under the same reaction conditions were used to evaluate each single pseudo-first-order constant together with experimental error.

Rate of $\text{TpivPP}\cdot\text{Fe}^{\text{II}}(\text{O}_2)(\text{M-MeIm})_2$ Decrease. Effect of Colloidal Platinum Concentration. The rates were measured under the conditions listed below: [iron porphyrin] = 9.10×10^{-6} M, [*N*-MeIm] = 1.60×10^{-4} M, [HCl] = 3.06×10^{-5} M, [Pt/PVP] = $(1.09\text{--}6.57) \times 10^{-10}$ particle equiv/L, $\text{H}_2/\text{O}_2 = 7:1$, toluene/ethanol = 2:1 (v/v), $T = 25 \pm 0.5$ °C. From the pseudo-first-order rates observed, apparent rate constants were obtained in accord with eq 1. Here \bar{k}^0 is a rate constant

$$k_{\text{obsd}}^{\text{Pt}} = \bar{k}^0 + k_{\text{Pt}}[(\text{Pt})_x/\text{PVP}] \quad (I)$$

obtained from the measurements in the absence of colloidal platinum. Under the present conditions, \bar{k}^0 is negligible small compared with the second term.

Measurements of K^{B} , K^{BB} , $K_{\text{O}_2}^{\text{B}}$, and $K_{\text{O}_2}^{\text{BB}}$. $\text{TpivPP}\cdot\text{Fe}^{\text{II}}\cdot\text{Cl}$ (10 mg) was dissolved in 10 mL of toluene, and into the solution 0.5 mL of H_2O was added. The mixture was deoxygenated by freeze–thaw cycles (4 times, 3×10^{-6} torr), and 100 mg of fine solid $\text{Na}_2\text{S}_2\text{O}_4$ was added to the mixture under Ar in the drybox. The mixture was stirred vigorously for 3 h. After reduction was complete, the toluene layer was separated and dried with anhydrous Na_2SO_4 . Toluene solution (0.075 mL, 9.1×10^{-4} M) of $\text{TpivPP}\cdot\text{Fe}^{\text{II}}$ was taken out and placed in a 5-mL flask to which 0.015–4.9 mL of a 1.87×10^{-3} M deoxygenated toluene solution of *N*-methylimidazole were added. Then the total volume was adjusted to 5 mL with addition of deoxygenated toluene under Ar. Deoxygenated ethanol (1 mL) and 2 mL of the toluene solution of $\text{TpivPP}\cdot\text{Fe}^{\text{II}}$ and *N*-methylimidazole prepared above were combined in a degassed cell for visible spectroscopy. Then, visible spectra were recorded at 25 °C in the 350–750-nm range. Base-binding equilibrium constants for $\text{TpivPP}\cdot\text{Fe}^{\text{II}}$ were determined by visible spectrophotometric titration at 535 and 555 nm. Dioxygen-binding equilibrium constants for $\text{TpivPP}\cdot\text{Fe}^{\text{II}}(\text{N-MeIm})_2$, EtOH, $K_{\text{O}_2}^{\text{B}}$, and for $\text{TpivPP}\cdot\text{Fe}^{\text{II}}(\text{N-MeIm})_2$, $K_{\text{O}_2}^{\text{BB}}$, were determined at 430 nm. Toluene–ethanol solutions containing $\text{TpivPP}\cdot\text{Fe}^{\text{II}}$ (9.1×10^{-6} M) and *N*-methylimidazole (1.2×10^{-5} , 5.7×10^{-5} , or 1.0×10^{-3} M) were prepared by the same procedures as above. 2-O_2 was formed by the gas exchange from Ar to $\text{N}_2\text{--O}_2$ mixed gas through freeze–thaw cycles by the use of a vacuum line (4 times, 3.0×10^{-6} torr) and refilling with $\text{N}_2\text{--O}_2$ of appropriate volume ratio. The N_2/O_2 ratio was determined by GLC under the conditions described previously.

Effect of Partial Pressure of Dihydrogen on the Rates. The rates were measured under the conditions listed below: [iron porphyrin] = 9.10×10^{-6} M, [*N*-MeIm] = 1.60×10^{-4} M, [HCl] = 3.06×10^{-5} M, [(Pt) $_x$ /PVP] = 2.19×10^{-10} particle equiv/L, $\text{H}_2/\text{O}_2/\text{N}_2 = (7\text{--}2):1:(0\text{--}5)$, toluene/ethanol = 2:1 (v/v), $T = 25 \pm 0.5$ °C;

$$k_{\text{obsd}}^{\text{H}_2} = k^0 + k_{\text{H}_2}P_{\text{H}_2} \quad (II)$$

From the pseudo-first-order rates observed, apparent rate constants were

Table V

| | [HCl], M | [N-MeIm], M | H_0 | h |
|---|-----------------------|-----------------------|-------|-----------------------|
| 1 | 1.02×10^{-4} | 1.60×10^{-3} | 7.94 | 1.15×10^{-8} |
| 2 | 3.06×10^{-4} | 1.60×10^{-3} | 7.32 | 4.79×10^{-8} |
| 3 | 6.12×10^{-4} | 1.60×10^{-3} | 6.93 | 1.17×10^{-7} |
| 4 | 9.18×10^{-4} | 1.60×10^{-3} | 6.64 | 2.29×10^{-7} |
| 5 | 12.2×10^{-4} | 1.60×10^{-3} | 6.35 | 4.47×10^{-7} |

obtained where k° is a rate constant obtained from rate measurements in the absence of dihydrogen. Known volumes of H_2 , O_2 , and N_2 were taken from a gas buret and fed into a 2-L gasbag which was connected to the 9-mL cell through a stopcock.

Effect of Hydrogen Chloride Concentration. The rates were measured under the conditions listed below: [iron porphyrin] = 9.10×10^{-6} M, [N-MeIm] = 1.60×10^{-3} M, [HCl] = $(1.02-12.2) \times 10^{-4}$ M, [(Pt)_x/PVP] = 2.19×10^{-10} particle equiv/L, $H_2/O_2 = 1:1$, toluene/ethanol = 2:1 (v/v), $T = 25 \pm 0.5$ °C. From the pseudo-first-order rate constants measured at the different imidazolium concentration (or acidity function), the following equation was derived, $k_{\text{obsd}}^{H^+} = k_{\text{obsd}}' + k_{H^+}[H^+]$

Values of $k_{\text{obsd}}^{H^+}$ were obtained from the plot of logarithms of the absorbance change vs. time. A value of k_{obsd}' was obtained from the measurements in the absence of the imidazolium ion. Acidity functions H_0 and h were determined by usual spectroscopic¹⁶ method where papaverine hydrochloride ($pK_a = 6.40$) was used as an indicator. The relationship between H_0 or h and the concentration of the imidazolium chloride is shown in the Table V.

Effect of the N-Methylimidazole Concentration. The effect of the concentration of N-methylimidazole on the rates was investigated under the conditions listed below: [iron porphyrin] = 9.10×10^{-6} M, [N-MeIm] = $(0.182-16.2) \times 10^{-4}$ M, [HCl] = $(0.06-6.0) \times 10^{-4}$ M, [(Pt)_x/PVP] = 2.19×10^{-10} particle equiv/L, $H_2/O_2 = 1:1$, toluene/ethanol = 2:1 (v/v), $T = 25 \pm 0.5$ °C. The ratio of N-methylimidazole concentration and the corresponding imidazolium chloride concentration was kept constant, and the total imidazole concentration was varied. Under these conditions, H_0 did not change and the effect of free N-methylimidazole concentration was studied.

Effect of Cyclohexene Concentration. Rates were measured by changing the concentration of cyclohexene under the conditions listed below: [iron porphyrin] = 9.10×10^{-6} M, [N-MeIm] = 1.60×10^{-4} M, [HCl] = 3.06×10^{-5} M, [(Pt)_x/PVP] = 2.19×10^{-10} particle equiv/L, [cyclohexene] = $(0-5.43) \times 10^{-3}$ M, $H_2/O_2 = 1:1$, toluene/ethanol = 2:1 (v/v), $T = 25 \pm 0.5$ °C. Cyclohexene was added to the iron porphyrin solution before the porphyrin solution was mixed with the platinum solution. The cyclohexene concentration did not affect the rate, but it affected the recycling number and the extent of decomposition of the catalyst.

Effect of Benzoic Anhydride Concentration in the Absence of Hydrogen Chloride. The rates were measured under the conditions listed below: [iron porphyrin] = 9.10×10^{-6} M, [N-MeIm] = 1.60×10^{-4} M, [(PhCO)₂O] = $(0-2.66) \times 10^{-3}$ M, [(Pt)_x/PVP] = 2.19×10^{-10} particle equiv/L, $H_2/O_2 = 1:1$, toluene/ethanol = 2:1 (v/v), $T = 25 \pm 0.5$ °C. Plot of time-logarithms of the absorbance at 544 nm gave a straight line in each kinetic run. The pseudo-first-order rate constant was determined and found to be independent of the benzoic anhydride concentration.

Effect of Benzoic Anhydride on the Product Yield. (Pt)_x/PVP in ethanol and a HCl/ethanol solution were prepared by the method described in the previous section. N-Methylimidazole (217 mg) was dissolved in 10 mL of toluene, and the solution was diluted to 2.64×10^{-3} M with toluene. TpivPP-Fe^{II}·(N-MeIm)₂ (11 mg) was dissolved in 25 mL of 7.0×10^{-4} M toluene solution of N-methylimidazole. In a typical reaction, the following reagents were placed in a 100-mL pear-shaped

flask equipped with a dropping funnel: 113 mg of benzoic anhydride (5.0×10^{-4} mol), 1 mL of 2.3×10^{-6} particle equiv/L ethanol solution of (Pt)_x/PVP (2.3×10^{-6} particle equiv), 5 mL of 4.18×10^{-3} M ethanol solution of HCl (2.0×10^{-5} mol), 10 mL of 2.64×10^{-3} M toluene solution of N-methylimidazole (2.64×10^{-5} mol), and 410 mg of cyclohexene (5.0×10^{-2} mol). In the dropping funnel was placed 2 mL of the 3.5×10^{-4} M toluene solution of TpivPP-Fe^{II}·(N-MeIm)₂ (7.0×10^{-7} mol).

At the top of the dropping funnel, a three-way stopcock was attached, and a 2-L gasbag containing a H_2-O_2 (1:1, v/v) mixed gas was attached to the three-way stopcock.

The solutions was saturated with the H_2-O_2 (1:1, v/v) mixed gas through repetition cycles of evacuation and refilling with the H_2-O_2 mixed gas, where more than 93% of TpivPP-Fe^{II}·(N-MeIm)₂ was converted to 2-O₂. Then the toluene solution of the 2-O₂ was added into the flask at once.

After vigorous stirring of the mixture for 30 min at room temperature, the H_2-O_2 mixture was replaced by Ar through several repeated cycles of evacuation and Ar refilling. A 4.4×10^{-3} M toluene solution of PhCO₂Me (2.2×10^{-5} mol) (5 mL) was added to the reaction mixture as an internal standard. The reaction mixture was then analyzed by GLC under the conditions described previously.

Kinetic Order with Respect to the Concentration of Iron Porphyrin. The rates were measured under the conditions listed below: [iron porphyrin] = $(4.55-13.5) \times 10^{-6}$ M, [N-MeIm] = 1.60×10^{-4} M, [HCl] = 3.00×10^{-5} M, [(Pt)_x/PVP] = 2.19×10^{-10} particle equiv/L, $H_2/O_2 = 1:1$, toluene/ethanol = 2:1 (v/v), $T = 25 \pm 0.5$ °C. Plot of time-logarithms of the absorbance at 544 nm gave a straight line in each kinetic run. The pseudo-first-order rate constant was determined and found to be constant for the different initial concentrations of iron porphyrin.

Reduction Rate of TpivPP-Fe^{III}-Cl by H₂-Colloidal Platinum. Rates of decrease of the TpivPP-Fe^{III}-Cl concentration were measured under the conditions listed below: [TpivPP-Fe^{III}-Cl] = 1.13×10^{-5} M, [N-MeIm] = 1.24×10^{-3} M, [HCl] = 6.00×10^{-5} M, [(Pt)_x/PVP] = $(1.09-4.38) \times 10^{-9}$ particle equiv/L, $P_{H_2} = 1$ atm, toluene/ethanol = 2:1 (v/v), $T = 25 \pm 0.5$ °C. The pseudo-first-order rate constants were obtained from plots of logarithms of the absorbance change at 507 nm vs. time at various concentration of colloidal platinum and iron porphyrin.

Products Analysis. Oxygenation of Cyclohexene (General Procedure). To a 100-mL pear-shaped flask equipped with a dropping funnel was added a toluene-ethanol solution (5:3, v/v, 16 mL) containing Pt/PVP, HCl, N-methylimidazole, cyclohexene, and PhCO₂Me as an internal standard for GLC analysis. In the dropping funnel was placed a toluene solution of TpivPP-Fe^{II}·(O₂)(N-MeIm) (3.5×10^{-4} M) and N-methylimidazole (7.0×10^{-4} M). After these solutions were saturated with H_2-O_2 (1:1) mixed gas, the toluene solution of the iron porphyrin was added at once. After the reaction mixture was stirred for the desired period of time at room temperature, the H_2-O_2 gas mixture was replaced by several repeated cycles of evacuation and refilling with Ar. The reaction mixture was then analyzed by GLC. 2-Ethoxycyclohexanol, 2-chyclohexen-1-one, and 2-chlorocyclohexanol (retention times of these compounds were 10.4, 7.5, and 17.4 min, respectively; poly(ethylene glycol) column, 3 mm diameter \times 2 m, 150 °C, N₂ carrier, 1.5 kg/cm²) were determined quantitatively on the basis of added PhCO₂Me standard.

During the treatment, TpivPP-Fe^{II}·(O₂)(N-MeIm) was converted to TpivPP-Fe^{III}-Cl. The amount of TpivPP-Fe^{III}-Cl was determined from the absorbance of TpivPP-Fe^{III}-Cl with electronic spectrophotometer. Reaction conditions and yields are shown in Table III.

Acknowledgment. Tabushi is very grateful to Prof. J. P. Collman, Stanford University, for his helpful discussion.